

# ***Ab initio* molecular-dynamics study of electronic and optical properties of silicon quantum wires: Orientational effects**

A. M. Saitta

*Istituto Nazionale per la Fisica della Materia, Scuola Internazionale Superiore di Studi Avanzati (SISSA),  
Via Beirut 2-4, I-34014 Trieste, Italy*

F. Buda

*Istituto Nazionale per la Fisica della Materia, Laboratorio Forum, Scuola Normale Superiore, Piazza dei Cavalieri 7, I-56126 Pisa, Italy*

G. Fiumara

*Istituto Nazionale per la Fisica della Materia, Unità di Ricerca di Messina, CP 50 I-98166 S. Agata, Messina, Italy*

P. V. Giaquinta

*Istituto Nazionale per la Fisica della Materia and Università degli Studi di Messina, Dipartimento di Fisica, Sezione di Fisica Teorica,  
CP 50 I-98166 S. Agata, Messina, Italy*

(Received 28 June 1995)

We analyze the influence of spatial orientation on the optical response of hydrogenated silicon quantum wires. The results are relevant for the interpretation of the optical properties of light-emitting porous silicon. We study (111)-oriented wires and compare the present results with those previously obtained within the same theoretical framework for (001)-oriented wires [F. Buda, J. Kohanoff and M. Parrinello, *Phys. Rev. Lett.* **69**, 1272 (1992)]. In analogy with the (001)-oriented wires and at variance with crystalline bulk silicon, we find that the (111)-oriented wires exhibit a direct gap at  $\mathbf{k}=0$ , the value of which is largely enhanced with respect to that found in bulk silicon because of quantum confinement effects. The imaginary part of the dielectric function, for the external field polarized in the direction of the axis of the wires, shows features that, while being qualitatively similar to those observed for the (001) wires, are not present in the bulk. The main conclusion which emerges from the present study is that, if wires a few nanometers large are present in the porous material, they are optically active independent of their specific orientation.

## **I. INTRODUCTION**

Silicon, one of the most relevant materials from the technological point of view, has excellent electronic properties as a semiconductor. However, in the crystalline form, it does not exhibit good optoelectronic properties because of the indirect gap, in the infrared range, between the valence and the conduction bands, and of the low probability of radiative electron-hole recombination. However, it is possible to modify deeply such properties using a process of electrochemical etching,<sup>1</sup> which produces a material known as light-emitting porous silicon (LEPS). This form, because of its luminescence properties, is presently the object of great scientific and technological attention.<sup>2</sup> In fact, inside this material, one can observe some wire structures: the wires are strictly interconnected with each other, and have a mean diameter of a few tens of angstrom. Quantum confinement of charge carriers seems to be at the origin of the optical characteristics of the material, which are quite different from those of bulk silicon.

In the recent past, many different theoretical studies<sup>3-10</sup> have been developed with the aim of analyzing the actual validity of the quantum confinement hypothesis, in order to explain those optical effects. According to the current experimental evidence, besides the presence of nanostructures of reduced dimensionality (wires and/or dots), the key ingredients that are necessary to induce luminescence are crystallin-

ity and surface passivation of dangling bonds. In the present work, we concentrate on the quantum wire model proposed to explain the optical properties of LEPS. We use the *ab initio* molecular dynamics (AIMD) method, as proposed by Car and Parrinello,<sup>11-13</sup> to study silicon quantum wires oriented along the (111) crystallographic direction. The AIMD method has been successfully applied to a variety of different systems and problems.<sup>12</sup> Porous silicon samples grown on a silicon substrate in the (111) lattice direction were characterized both in the morphology and in the optical properties.<sup>14-16</sup> The study presented here follows a similar work developed for quantum wires oriented along the (100) crystallographic direction.<sup>3</sup> This study showed the presence of a direct gap in the visible range and an important enhancement of the dipole-matrix elements, which are directly related to the transition probability between the valence and the conduction band and, in consequence of that, to the absorption coefficient. This work, such as all the others quoted above, shows how the optical and electronic properties of silicon become deeply modified by quantum confinement. These predictions, with the limitations due to the local density approximation (LDA) used in the AIMD framework, support the thesis that the origin of porous silicon photoluminescence lies in the localization of charge carriers inside ordered structures of reduced dimensionality.

The present work tries mainly to ascertain if the orientation may be relevant in determining the optical and elec-

tronic properties of the material since, *a priori*, it is not obvious that charge carriers confinement acts in a similar way along different symmetry planes. In Sec. II, we describe the geometry of the model used and give some computational details. In Sec. III, the results on the structural, vibrational, and electronic properties of the model are discussed. The final section is devoted to the conclusions.

## II. SILICON WIRE GEOMETRY AND TECHNICAL DETAILS

Crystalline silicon is characterized by a diamond structure, in which atoms are distributed in a face centered cubic (fcc) lattice, each lattice site being occupied by a pair of particles, the chemical bond, about  $2.35 \text{ \AA}$  long, of which lies in the (111) direction. The silicon lattice structure along the (111) direction can be characterized by three double layers periodically repeated with a periodicity  $a\sqrt{3}$ , where  $a$  is the lattice parameter of bulk crystalline silicon ( $5.43 \text{ \AA}$ ). Figure 1 shows the smallest wire that one can build, still preserving the crystalline order along the (111) direction. The unit cell, indefinitely replied in space through periodic boundary conditions, contains 26 silicon atoms, plus 30 hydrogen atoms, which are necessary to saturate the dangling bonds at the surface of the wire. The geometry of the model is such that it exhibits a nonuniform size along the longitudinal direction. In a way, this feature makes the model more similar to real samples of porous silicon. In fact, the diameter of the model has a maximum value of  $7.67 \text{ \AA}$ , and a mean value of  $5.51 \text{ \AA}$ . We have also studied a larger wire, the basic structure of which consists of 62 silicon atoms and 42 hydrogen atoms, with a maximum diameter of  $11.72 \text{ \AA}$ , and a mean value of  $10.37 \text{ \AA}$ . We note that a system consisting of 104 atoms is rather demanding on the computational side for *ab initio* Car-Parrinello simulations. For this reason, we limited our calculations for the larger wire to those features that may confirm some specific properties of the thinner wire. In both cases, the size of the supercell in the longitudinal direction corresponds exactly to the bulk silicon characteristic size of  $9.41 \text{ \AA}$  along the (111) direction. The lateral size of the supercell is much larger than the diameter of the wire, so as to avoid interactions of the particles with their images. The parameters needed in the AIMD simulation were suggested by the previous experience on this material: we used a time step of 7 a.u., an energy cutoff for the plane-wave expansion of 8 Ry, an electronic mass of 300 a.u., and pseudopotentials of the Bachelet-Hamann-Schluter<sup>17</sup> type for describing the interaction between valence electrons and the nuclei with core electrons.

## III. RESULTS

### A. Structural relaxation and vibrational properties

As a first step, we wanted to verify the structural stability of the wire. To this aim, after the electronic ground-state relative to the initial ionic configuration was found, we let all the ionic degrees of freedom relax with a steepest descent technique. We notice a small increase of the distance of the most external atoms from the axis of the wire, of the order of  $0.16 \text{ \AA}$ , analogously to what was observed in Ref. 3 As expected, we observe no relevant variations of the characteris-

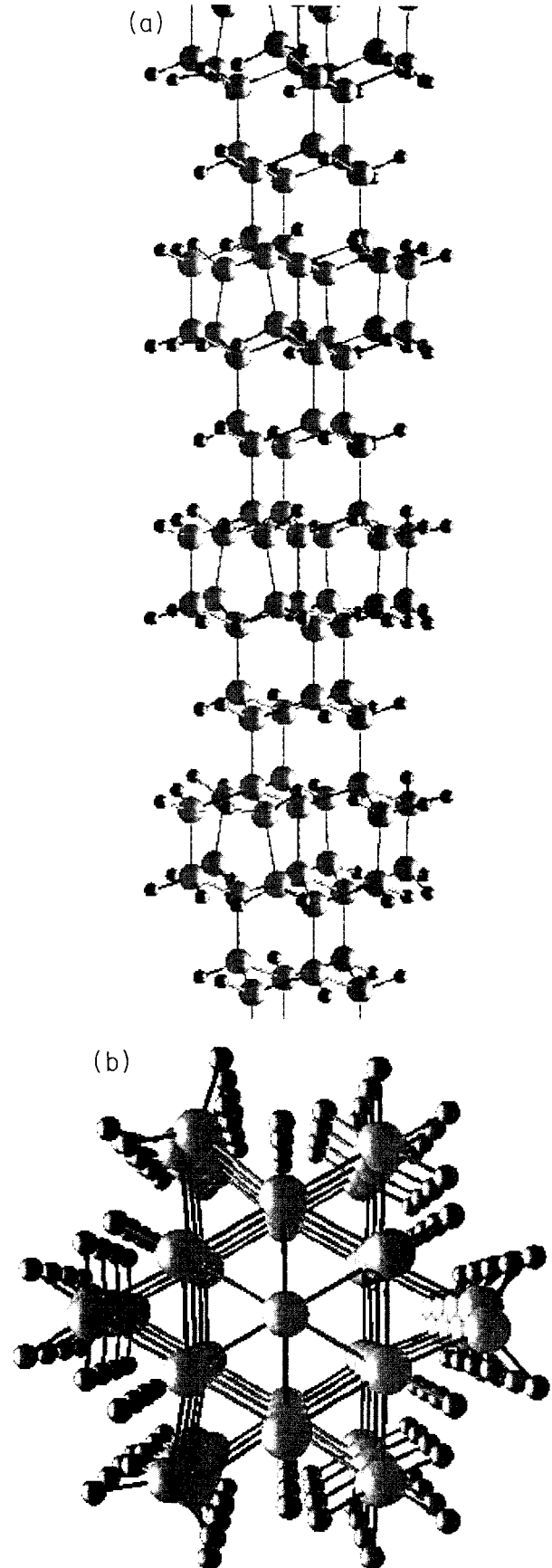


FIG. 1. Silicon quantum wire oriented in the (111) direction: side view [panel (a)] and top view [panel (b)]. The large balls represent silicon atoms, while the small balls indicate the hydrogen atoms passivating the dangling bonds at the surface of the wire.

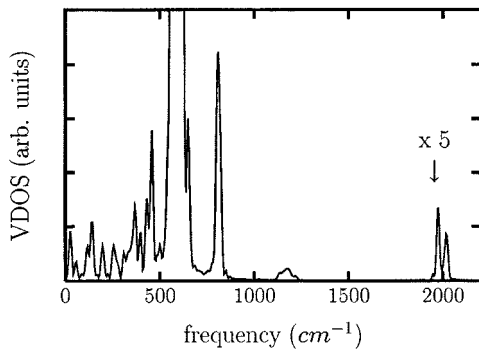


FIG. 2. Vibrational spectrum for a (111)-oriented wire with an average diameter of 5.51 Å. We rescaled a factor of 5 the feature at about 2000  $\text{cm}^{-1}$ , in order to emphasize the double peak (see text).

tic distances, along the longitudinal direction. Then, we let the system evolve dynamically for a time of about 2 ps, a considerable time in AIMD, so that one may be confident that the system is reasonably close to thermal equilibrium. During this evolution, the model did not exhibit any pathological behavior: the system oscillates about the equilibrium configuration with no substantial atomic rearrangements. We observe that the total energy (potential + kinetic) fluctuates around an average value that remains constant, as should be in a microcanonical AIMD simulation. The average temperature during this dynamical evolution is about 70 K.

We also computed the velocity autocorrelation function and, through its Fourier transform, an indicative vibrational density of states of the system. We find good qualitative agreement with the typical experimental data of the vibrational modes of Si-Si and Si-H bonds.<sup>18</sup> From a strictly quantitative point of view, we remark that the relative intensity of the peaks should not be taken too rigorously. However, the positions of the peaks are in fair agreement with the experimental data. In particular, we recognize, in the spectra of Fig. 2, the characteristic signal of the stretching of the Si-H bond at about 2000  $\text{cm}^{-1}$ . The double peak has its origin in the presence of doubly hydrogenated silicon atoms, which give rise to symmetrical and antisymmetrical stretching of the bond at slightly different frequencies. The analysis of the oscillations of single and twin hydrogen particles shows that the higher-frequency peak can be ascribed to the symmetrical mode, while the lower-frequency signal arises from antisymmetrical stretching vibrations. We notice also, at lower frequencies, the typical signals of scissors mode (800  $\text{cm}^{-1}$ ) of the twin hydrogen atoms bonded to one silicon atom, and of Si-H bending (around 600  $\text{cm}^{-1}$ ). The weak structure centered at about 1150  $\text{cm}^{-1}$  is likely associated with another bending vibrational mode of hydrogen atoms, as it shows up in the motion of both single and twin passivating hydrogens. The low-frequency noise produced by the finite time evolution renders more uncertain the identification of the modes below 500  $\text{cm}^{-1}$  that are associated with the motion of silicon atoms. It is important to remark that such characteristic vibrational modes are observed, by infrared spectroscopy, also in real freshly prepared LEPS samples.<sup>18</sup>

For the larger-size sample, we have also studied the relaxation towards the global energy minimum. It is noteworthy that, in this case, the mean radial relaxation, in the equilibrium configuration, is negligibly small if compared with that

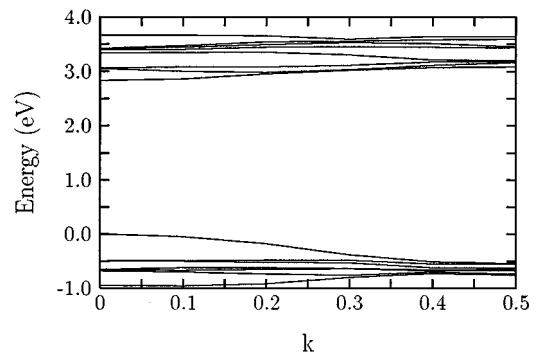


FIG. 3. Electronic band structure for the smaller (111)-oriented wire along the one-dimensional Brillouin zone. We express  $k$  in units of  $2\pi/c$ , where  $c$  is the periodicity along the direction of the wire. Only a few bands close to the energy gap are plotted.

estimated for the thinner wire. This can be intuitively understood if one thinks that in the smaller-size model the ratio of surface to bulk atoms is definitely higher than in the larger wire. Such a small relaxation originates from the competition between the doubly hydrogenated silicon atoms, which move slightly away from the axis of the wire, and the singly hydrogenated ones, which instead move inward.

## B. Electronic and optical properties

Once the minimum energy configuration has been determined, we computed the electronic band structure of the quantum wire along the one-dimensional Brillouin zone (BZ). We computed the Kohn-Sham eigenvalues for six different  $k$  points of the BZ, from the center ( $\Gamma$ ) to the border (which would correspond to  $L$  in the bulk). The resulting band structure is shown in Fig. 3, for the (111)-oriented wire, with a mean diameter of 5.51 Å. The main result is the prediction of a direct gap of 2.83 eV between the conduction and the valence band at the zone center. It is also interesting to notice that the second conduction state still shows a signature of the band structure of bulk silicon, i.e., a minimum located at about 0.2. As to the gap, we recall that Buda and co-workers found, for a (100)-oriented quantum wire with a diameter of 7.60 Å, a value of 2.33 eV.<sup>3</sup> The difference is to

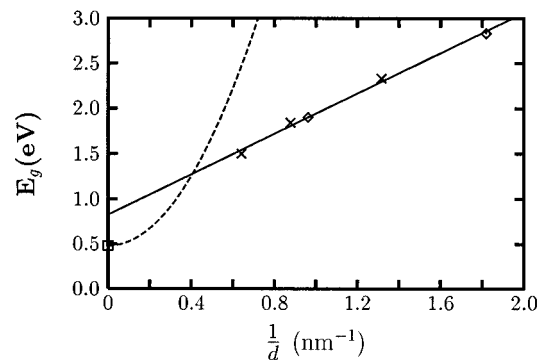


FIG. 4. Computed energy gap, as a function of the inverse wire diameter. We show both the (111) wires (diamonds) and (100) wires (crosses) computed gap. The full line is the linear fit to this points. The dashed curve represents the effective mass theory prediction. The LDA bulk silicon gap is represented by the square on the vertical axis.

TABLE I. Square modulus of the transverse and longitudinal dipole-matrix elements for the smaller wire in units of bohr<sup>-2</sup>. The top of the valence band and the bottom of the conduction band are labeled by indices 67 and 68, respectively.  $E_c - E_v$  is the difference between the conduction and valence Kohn-Sham eigenvalues.

$N_c$	$N_v$	$ \langle \psi_{c,n_c}   \mathbf{e} \cdot \mathbf{p}   \psi_{v,n_v} \rangle_{\perp} ^2$	$ \langle \psi_{c,n_c}   \mathbf{e} \cdot \mathbf{p}   \psi_{v,n_v} \rangle_{\parallel} ^2$	$E_c - E_v$ (eV)
68	65	$0.50 \times 10^{-3}$	$0.11 \times 10^{-1}$	3.33
68	66	$1.00 \times 10^{-3}$	$0.14 \times 10^{-1}$	3.32
68	67	$0.23 \times 10^{-5}$	$0.86 \times 10^{-3}$	2.83
74	67	$0.42 \times 10^{-3}$	$0.17 \times 10^{-1}$	3.42
76	67	$0.94 \times 10^{-2}$	$0.45 \times 10^{-1}$	3.67

be ascribed, as we shall see later, to the different mean diameter of the two models, more than to the different symmetry of the wires. We recall that in bulk silicon, the minimum of the conduction band along the  $\Gamma$ - $L$  direction falls just at  $L$ , with a gap of 2.15 eV.

For the larger wire, we find an energy gap of 1.90 eV at the center of BZ which, consistently with the quantum confinement hypothesis, is larger than that in bulk silicon, but smaller than the value for the thinner wire. The values of the two energy gaps, together with those of the (100) models and of bulk silicon as obtained in LDA, are plotted in Fig. 4. The linear behavior of the energy gap, as a function of the inverse size of the models, is of striking evidence. It is remarkable that both the (111) and (100) computed values lie on the same straight line, suggesting the independence of such a property on the specific orientation of the wires. In the same figure, we also show the theoretical prediction coming from effective mass arguments ( $E_g \sim 1/d^2$ ), which should hold close to the bulk limit. It appears that the matching between these two different behaviors should occur in the region between 2 and 5 nm.

The presence of a direct gap, and thus the possibility of zero-phonon transitions, is not a sufficient condition for ensuring good photoluminescence properties. The probability of an electronic transition as a result of the absorption of a photon is given by the Fermi golden rule, which, in the dipole approximation, is  $|\langle \psi_{c\mathbf{k}} | \mathbf{e} \cdot \mathbf{p} | \psi_{v\mathbf{k}} \rangle|^2$ , where  $\psi_{c\mathbf{k}}$  and  $\psi_{v\mathbf{k}}$  are the conduction and valence states involved in the electronic transition, while  $\mathbf{e}$  is the polarization vector and  $\mathbf{p}$  the momentum operator. We determined all the matrix elements between the Kohn-Sham states of the conduction and valence bands, the difference in energy of which falls in the

visible range, or slightly above it. Table I and Table II give the values of the most relevant of these dipole-matrix elements for the smaller and the larger (111)-oriented wires. We note the strong difference between the values relative to the longitudinal and transverse polarizations. Moreover, the quantum confinement of the electrons mixes up the states, thus allowing for transitions that are forbidden in the bulk by selection rules. The dipole-matrix element between the top of the valence band and the bottom of the conduction band is not zero because of the mixing, even though it is not very large.

We computed the imaginary part of the dielectric function, that is related to the absorption coefficient, through the formula

$$\epsilon_2(\omega) = \frac{4\pi^2 e^2}{m^2 \omega^2} \frac{L_w}{V} \sum_{v,c} \int_{\text{BZ}} \frac{2 dk_z}{2\pi} |\langle \psi_{c k_z} | \mathbf{e} \cdot \mathbf{p} | \psi_{v k_z} \rangle|^2 \times \delta[E_c(k_z) - E_v(k_z) - \hbar\omega] \quad (1)$$

where  $L_w$  and  $V$  are the length of the wire and the volume of the supercell, respectively. The results for the smaller model are shown in Fig. 5. In the construction of this quantity, we have considered only the dipole-matrix elements corresponding to energy differences up to 4 eV. We observe that the component related to an external field parallel to the wire direction is much stronger than the perpendicular one, and this difference becomes larger and larger going to lower energies. Probably, the most interesting result is the presence, in the parallel component, of a small signal at the band gap (2.83 eV), which is completely absent in the perpendicular one. This is a clear effect of the mixing of the bulk states

TABLE II. Square modulus of the transverse and longitudinal dipole-matrix elements for the larger wire in units of bohr<sup>-2</sup>. The top of the valence band and the bottom of the conduction band are labeled by indices 145 and 146, respectively.  $E_c - E_v$  is the difference between the conduction and valence Kohn-Sham eigenvalues.

$N_c$	$N_v$	$ \langle \psi_{c,n_c}   \mathbf{e} \cdot \mathbf{p}   \psi_{v,n_v} \rangle_{\perp} ^2$	$ \langle \psi_{c,n_c}   \mathbf{e} \cdot \mathbf{p}   \psi_{v,n_v} \rangle_{\parallel} ^2$	$E_c - E_v$ (eV)
147	138	$0.17 \times 10^{-4}$	$0.12 \times 10^{-1}$	2.84
148	139	$0.18 \times 10^{-4}$	$0.12 \times 10^{-1}$	2.84
146	145	0	$0.41 \times 10^{-3}$	1.90
156	145	$0.36 \times 10^{-5}$	$0.14 \times 10^{-1}$	2.83
167	145	$0.17 \times 10^{-4}$	$0.57 \times 10^{-1}$	3.34
168	145	$0.11 \times 10^{-2}$	$0.23 \times 10^{-1}$	3.36
171	145	$0.17 \times 10^{-1}$	$0.11 \times 10^{-1}$	3.44

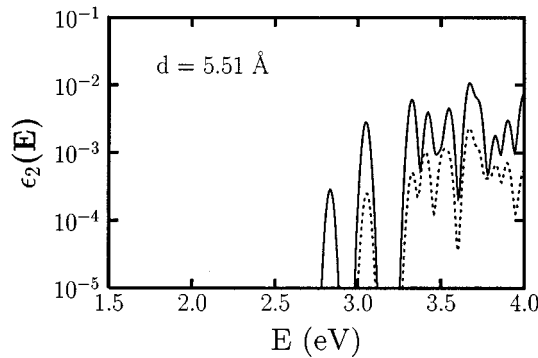


FIG. 5. Imaginary part of the dielectric function  $\epsilon_2(E)$  for the thinner wire. The plot is on a semilogarithmic scale. The full line represents  $\epsilon_2^{\parallel}$ , while the dashed line refers to  $\epsilon_2^{\perp}$ .

induced by the reduced dimensionality. This result seems to be peculiar of the (111) wire, since in the (100) models,<sup>3</sup> the dipole-matrix element between the top of the valence band and the bottom of the conduction band was negligible in both the components.

The plot of the dielectric function for the larger-sized wire, that is shown in Fig. 6, exhibits also a different behavior in the parallel and the perpendicular components. We notice also, in this case, a clear difference in intensity between the parallel and the perpendicular components at higher energies. The most remarkable feature is the presence, below  $\sim 2.7$  eV, of three peaks in the longitudinal component that are not observed in the transverse one. In particular we observe again a significative signal in the correspondence of the energy gap (1.90 eV), the intensity of which is lowered with respect to the smaller wire. This is consistent with the fact that in the bulk limit, this matrix element should go to zero.

#### IV. CONCLUSIONS

We have presented an electronic structure calculation, within the LDA, of two (111)-oriented silicon quantum wires of different size. The comparison of the present results with those obtained for the (001)-oriented models shows a substantial analogy of the electronic and optical properties of silicon quantum wires oriented along different crystallo-

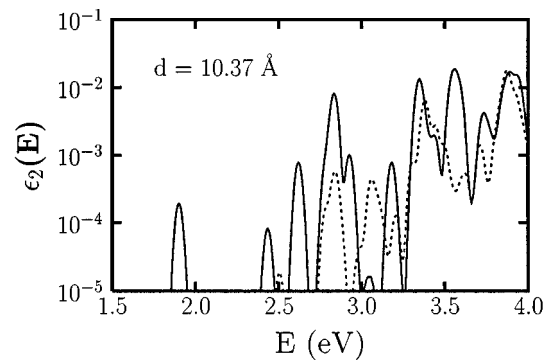


FIG. 6. Imaginary part of the dielectric function  $\epsilon_2(E)$  for the larger wire. The plot is on a semilogarithmic scale. The full line represents  $\epsilon_2^{\parallel}$ , while the dashed line refers to  $\epsilon_2^{\perp}$ .

graphic directions. In particular we find a direct energy gap at the zone center, the magnitude of which decreases for larger wires consistently with the quantum confinement hypothesis. Quite surprisingly, we find that the values of the gap for all the (111) and (001) wires studied are excellently fitted as a linear function of the inverse diameter. Therefore, this quantity seems to be independent of the orientation and geometrical details, and is affected only by the width of the wire. Again, the present calculations support the idea that the photoluminescence properties of porous silicon can be ascribed to charge carriers confinement in nanostructures. We find, similarly to the (001) wires, a strong anisotropy in the imaginary part of the dielectric function. These results indicate that, if the LEPS structure consists of a network of randomly oriented wires,<sup>19</sup> all of them will contribute to the photoluminescence independent of their specific orientation.

#### ACKNOWLEDGMENTS

This work was supported by the Ministero dell'Università e della Ricerca Scientifica e Tecnologica (MURST) and by the Istituto Nazionale per la Fisica della Materia (INFN), Italy. The authors thank the Centro di Calcolo Elettronico dell'Università degli Studi di Messina for the allocation of computer time. A.M.S. would also like to acknowledge the hospitality of the IBM-ECSEC centre in Rome in the early stage of this work. Very useful discussions with J. Kohanoff, S. Ossicini, and O. Bisi are also acknowledged.

<sup>1</sup>A. Uhlir, Bell Syst. Tech. J. **33**, 333 (1956).

<sup>2</sup>L. T. Canham, Appl. Phys. Lett. **57**, 1046 (1990).

<sup>3</sup>F. Buda, J. Kohanoff, and M. Parrinello, Phys. Rev. Lett. **69**, 1272 (1992).

<sup>4</sup>F. Buda and J. Kohanoff, Prog. Quantum Electron. **18**, 201 (1994).

<sup>5</sup>M. S. Hybertsen and M. Needels, Phys. Rev. B **48**, 4608 (1993).

<sup>6</sup>A. J. Read, R. J. Needs, K. J. Nash, L. T. Canham, P. D. J. Calcott, and A. Qteish, Phys. Rev. Lett. **69**, 1272 (1992).

<sup>7</sup>T. Ohno, K. Shiraishi, and T. Ogawa, Phys. Rev. Lett. **69**, 2400 (1992).

<sup>8</sup>B. Delley and E. F. Steigmeier, Phys. Rev. B **47**, 1397 (1993).

<sup>9</sup>M. S. Hybertsen, Phys. Rev. Lett. **72**, 1514 (1994).

<sup>10</sup>O. Bisi and S. Ossicini, Phys. Rev. B (to be published).

<sup>11</sup>R. Car and M. Parrinello, Phys. Rev. Lett. **55**, 2471 (1985).

<sup>12</sup>G. Galli and M. Parrinello, *Computer Simulation in Material Science* (Kluwer, Dordrecht, 1991), pp. 283–304.

<sup>13</sup>G. Pastore, E. Smargiassi, and F. Buda, Phys. Rev. A **44**, 6334 (1991).

<sup>14</sup>V. A. Karavanskii, M. A. Kachalov, A. P. Maslov, Yu N. Petrov, V. N. Seleznev, and A. O. Shuvalov, Pis'ma Zh. Éksp. Teor. Fiz. **57**, 229 (1993) [JETP Lett. **57**, 239 (1993)].

<sup>15</sup>V. S. Dneprovskii, V. A. Karavanskii, V. I. Klimov, and A. P. Maslov, Pis'ma Zh. Éksp. Teor. Fiz. **57**, 394 (1993) [JETP Lett.

- 57**, 406 (1993)].
- <sup>16</sup>C. H. Perry, F. Lu, F. Namavar, N. M. Kalkhoran, and R. A. Soref, Appl. Phys. Lett. **60**, 3117 (1992).
- <sup>17</sup>G. B. Bachelet, R. D. Hamann, and M. Schlüter, Phys. Rev. B **26**, 4199 (1982).
- <sup>18</sup>M. A. Tischler and R. T. Collins, Solid State Commun. **84**, 819 (1992).
- <sup>19</sup>R. Tsu, H. Shen, and M. Dutta, Appl. Phys. Lett. **60**, 112 (1992).